Tellus (1985), *37B*, 272–285

Modelling of gas flux through bubbles at the air-water interface

By LAURENT MEMERY and LILIANE MERLIVAT, *Laboratoire de Géochimie Isotopique, IRDI/DPC/CEN-Saclay, 91191 Gif Sur Yvette Cedex, France*

(Manuscript received February, 1, 1984; in final form July 30, 1985)

ABSTRACT

A theoretical approach to gas transfer by bubbles created by breaking waves at the air-water interface is undertaken. Based on a simple model, this study affords a basic understanding of the physical mechanisms. The behaviour of a single bubble is examined. Similarities and differences between the formulation of gas fluxes across a "flat" air-water interface and through bubbles are shown. The gas flux through bubbles is not strictly proportional to the solubility and to the difference of concentrations between the bulk of the water and the surface. Nevertheless, for trace gases, a linear relationship with this difference of concentrations, increasing with solubility is predicted. Overpressure in the bubbles and dissolution favour invasion into the water and imply a water supersaturation at equilibrium. This supersaturation is more important when the gas solubility is low. The rôle of surfactants is studied and it is found that they can reduce the gas exchange by a factor of 5. The consequences of the model for the transfer velocity are briefly presented. A better definition of the bubble lifetime, i.e., a better representation of water dynamics under a breaking wave, is necessary to make more reliable model predictions, most importantly for gases with low solubility. Theoretical studies on the bubble source are necessary in order to avoid, as far as possible, the use of the bubble distribution.

1. Introduction

Until now, most of the models dealing with gas transfer across an air-water interface have been concerned with moderate wind regimes. A molecular-eddy diffusivity concept has been used. The relationship between the transfer velocity k_L and different parameters describing the gas considered and the hydrodynamical conditions at the interface thus takes the following shape: $k_L \sim Sc^{-n} u_*$, where u_* is the friction velocity and Sc the Schmidt number ($Sc = \nu/D$; ν is the viscosity of the water and D the gas molecular diffusion coefficient) (Hasse and Liss, 1980). The value of n is equal to $\frac{2}{3}$ for Deacon's (1977) film model and to $\frac{1}{2}$ for the surface renewal model. Using results of gas transfer measurements in wind-wave facility, Jahne et al. (1984) found that n varies between $\frac{2}{3}$ for low wind speeds and $\frac{1}{2}$ when the wind becomes higher.

In ocean conditions, waves often break which implies changes in the interface conditions, an increase in the turbulence and the creation of air bubbles in the bulk of water. From a theoretical point of view, little is known about these aspects of gas transfer.

The change in the state of the interface and its influence on gas exchange has been studied in Kerman's (1984) model, describing a roughened sea characterized by patches of breaking waves. He used the model of Yaglom and Kader (1974) for heat and mass transfer between a rough wall and a turbulent fluid flow and applied it to a compliant surface. The relationship obtained for the transfer velocity is given by: $k_L \sim (Sc)^{-2/3} u_*^{5/2}$.

For the most part, the few previous studies on gas exchange and breaking waves have turned on the bubble contribution. With the help of his own acoustic measurements of bubble clouds in Loch Ness, Thorpe (1982) has developed a cell model for bubble dispersion to take into account the bubble entrainment in breaking wind waves. His work has been oriented towards air transfer: no specific gas

was considered in the bubbles. In his computations, a single bubble size has been used. This study has shown that the "natural" state of the water under the surface when there are bubbles is supersaturation and that the gas flux through bubbles can be significant for wind speeds of $12\ m \cdot s^{-1}$ and more. Siems (1980) and Merlivat and Memery (1983) have presented computations of transfer velocity in order to explain their own gas transfer results obtained during experiments run in wind wave facilities. These results show a large enhancement of the transfer velocity under conditions of high wind speeds and breaking waves. Moreover, this phenomenon is more pronounced for gases with low solubility. From a very simplified model adapted to his experimental conditions (water greatly supersaturated in CO_2-0.4 bar and O_2-0.3 bar) and with the bubble distributions measured by photographic methods, Siems explained the increase in CO_2 and O_2 transfer at high wind speeds. Contrary to Thorpe and Siems, no bubble measurements were done during the experiments of Merlivat and Memery. Their observations of N_2O and Ar exchanges have motivated a general study of gas transfer through bubbles, based on water dynamics described by irrotational orbital motions of Stockes. Turbulence and downward convection created by breaking waves are not taken into account. Principally centred on the notion of transfer velocity, this study has demonstrated the large influence of the solubility, the non-symmetry between evasion and invasion, the water supersaturation at equilibrium, when the bubbles are considered. Finally, this work questions the very notion of transfer velocity and its use in the measurements of gas fluxes.

The study we undertake now proceeds from a model of gas transfer through bubbles, taking into account the main different mechanisms involved. We establish a general and simplified formulation of the gas flux which allows an easy and physical understanding of its dependency on the most significant parameters. We emphasize the flux of trace gases, keeping in mind the problem of the uptake of the anthropogenic CO_2 (and other pollutants) by the ocean. Consequently, in addition to air, we consider simultaneously two trace gases. Moreover, different ranges in the bubble radius are taken into account, as are the differences between clean and dirty bubbles. The simplifications of the model are in the determination of the bubble lifetime: the waterflow created by breaking waves is not represented. This crucial problem is briefly discussed in the conclusion. The difference from gas transfer across a flat air-water interface is thoroughly examined.

2. Theory of gas transfer for single bubbles

2.1. General equations

2.1.1. Hypotheses. When a wave breaks, air is confined in the water: the bubbles formed are entrained by a strong downward waterflow. As the velocity field decays, the bubbles tend to rise under buoyancy.

The equations presented in this article describing the behaviour of the bubbles created by breaking waves are based on the following simplifying hypotheses.

—The bubbles are created instantaneously at their initial depth z_0 with their initial radius r_0 and with the same composition as the atmosphere from which they are formed: bubble descent time is assumed to be negligible.

—The bubbles rise at very nearly their terminal velocity: their initial acceleration is such that only a distance equal to some bubble radii is needed to reach a constant velocity (Garrettson, 1973).

2.1.2. Bubble dynamics. The regime of bubble motion varies considerably with the Reynolds number $Re = 2rw/\nu$, where ν is the viscosity of the water and w the ascent velocity of the bubble.

Downstream of the bubble, the changes in the structure of the flow are directly linked to the Reynolds number. According to its value, different formulations of the drag coefficient must be considered. Moreover, the nature of the interface bubble-water depends on the surface active materials contained in the water. The hydrodynamical conditions of the water surrounding the bubble change when the surface is assumed to be liquid (clean bubble) or solid (dirty bubble). For example, the velocity field becomes equal to zero at a solid liquid interface, whereas only the normal component of the velocity tends to zero at a liquid-liquid interface.

— Dirty bubbles behave like solid spheres. The drag coefficient C_D (ratio of the drag force F_D and of the product of $\frac{1}{2}\ \rho w^2$ by the area of the bubble

πr^2) is equal to:

$$\frac{24}{\mathrm{Re}}\left(1+\frac{3}{16}\mathrm{Re}\right) \quad \text{(Batchelor, 4–10, p. 244, 1967).}$$

The drag force F_D being counterbalanced by the buoyancy forces F_B ($=\frac{4}{3}\pi r^3 \rho g$), w satisfies the equation:

$$w^2 + \frac{8\nu}{3r}w - \frac{16}{27}rg = 0. \tag{1}$$

When Re tends to O, $C_D \to 24/\mathrm{Re}$, i.e. $F_D \to 6\pi r\rho\nu w$ and $w \to 2gr^2/9\nu$.

— For clean bubbles with small radii ($r < 100\ \mu$m), the drag is viscous (Levich, 81, p. 435, 1962).

$$F_D = 4\pi r\,\rho\nu w \quad \text{and} \quad w = \frac{1}{3}\frac{\mathrm{gr}^2}{\nu}. \tag{2}$$

When the radius becomes larger, the flow is separated on the downstream portion of the bubble surface. The drag coefficient is equal to:

$$\frac{48}{\mathrm{Re}}\left(1-\frac{2\cdot 2}{\mathrm{Re}^{1/2}}\right) \quad \text{(Batchelor, 5, 14, p. 368, 1967).}$$

w then satisfies:

$$w - 2.2\left(\frac{\nu}{2r}\right)^{1/2} w^{1/2} - \frac{gr^2}{9\nu} = 0. \tag{3}$$

With the approximation $C_D = 48/\mathrm{Re}$, it is found that $F_D = 12\pi r\rho\nu w$ and $w = gr^2/9\nu$.

For large Reynolds number (Re > 700), the bubble loses its spherical shape and w reaches a maximum value of 30 cm · s^{-1}.

Fig. 1 shows the relationship between the velocity of a bubble and its radius.

2.1.3 Bubble gas transfer. The gas transfer through a bubble is defined by the equation:

$$\frac{dn}{dt} = kr^2(c - sP_b), \tag{4}$$

where n is the amount of the gas considered in the bubble, k the transfer velocity, c the gas-concentration in the water, s the solubility of the gas and P_b its partial pressure in the bubble:

$P_b V = nRT$ with $V = \frac{4}{3}\pi r^3$ the volume of the bubble.

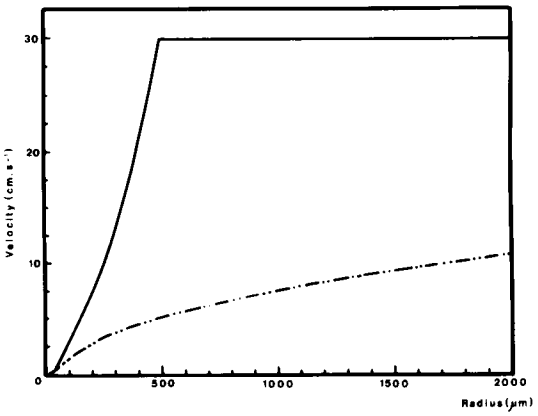

Fig. 1. Relationship between the ascent velocity and the bubble radius r. ——: clean bubble; —··—: dirty bubble.

For solid spheres,

$$k = 8\,(D^2 w/r^2)^{1/3} \tag{5}$$

(Levich, 14, p. 85, 1962).

For clean bubbles,

$$k = 8\,(\pi D w/6r)^{1/2} \tag{6}$$

for small Reynolds number (Levich, 91, p. 467, 1962).

$$k = 8\,(\pi D w/2r)^{1/2} \tag{7}$$

for $r > 500\ \mu$m (Levich, 91, p. 468, 1962).

D is the molecular diffusion coefficient in water.

The variation in k with the radius is shown in Fig. 2 for two gases: He and CO_2 (see Table 1, the physico-chemical properties of these gases).

2.1.4. Variation in bubble radius. In a bubble, $PV = (\Sigma n)\,RT$, with

$$P = P_0 - \rho gz + \frac{2\sigma}{r}. \tag{8}$$

P_0 is the atmospheric pressure, z the negative depth where the bubble is located and σ the surface tension ($\sigma \to 0$ for dirty bubbles).

After derivation, we obtained:

$$\frac{dr}{dt} = \frac{\dfrac{3RT}{4\pi r^2}\left(\sum\dfrac{dn}{dt} + r\rho gw\right)}{3P - 2\sigma/r}. \tag{9}$$

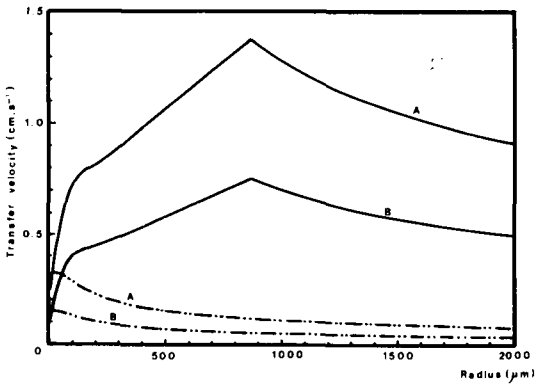

Fig. 2. Relationship between the transfer velocity k of a single bubble and the radius r. ——: clean bubble; —··—: dirty bubble. A: He. B: CO_2.

Table 1. *Physico-chemical properties at 20 °C (Broecker and Peng, 1974) and molar fractions in the air of different gases*

Gas	α*	D† $\times 10^5$	X_a
N_2	0.0155	1.71	0.79
O_2	0.0310	2.06	0.20
air‡	0.0188	1.78	1
CO_2	0.878	1.64	3.3×10^{-4}
Rn	0.242	1.20	10^{-19}
Ar	0.0367	1.56	10^{-2}
He	0.00868	5.48	5.4×10^{-6}

* $\alpha = sRT$ where s is the gas solubility defined by Henry's law: $c_e = sP$.
† In $cm^2 \cdot s^{-1}$.
‡ Air $\simeq 0.79\ N_2 + 0.2\ O_2 + 0.01$ Ar.

2.1.5. Definitions. The different gases considered in this study are air (20% of O_2 and 80% of N_2) and trace gases defined by a concentration lower than 10^{-3}.

The gas concentrations in water are assumed to be constant with time. This concentration is defined by the mole fraction $X_w : C = sP_w = sX_wP_0$:

$$x = \frac{X_w - X_a}{X_a}$$

is the water saturation indicator, where X_a represents the gas mole fraction in the air.

$$y = \frac{2\sigma/r - \rho g z}{P_0}$$

is the prevalent over-pressure in the bubble.

Gas transfer through a bubble can be entirely described by three main time constant:

— the lifetime: $\tau_l = -\dfrac{z_0}{w(r)}$; (10)

— the gas exchange time constant

$$\tau_g = \frac{4\pi r}{3\alpha k}; \quad (11)$$

with $\alpha = sRT$

— the radius time constant τ_r.

Assuming the air to be in equilibrium in solubility ($X'_w = X'_a = X'_b = 1$, where the prime index refers to air and X_b is the gas mole fraction in the bubble), using eq. (4) we find:

$$\frac{dn'}{dt} = -s' P_0 k' r^2 y.$$

Furthermore, the total amount of trace gases in a bubble is negligible, compared with the amount of air n'. Thus, $\Sigma n \simeq n'$.

We can define a radius constant time by:

$$\tau_r = \frac{r}{dr/dt} = \tau'_g \frac{3P - 2\sigma/r}{P_0/(\eta' - y)}, \quad (12)$$

where

$$\eta' = \tau'_g/\tau_p, \qquad \tau_p = P_0/\rho g w. \quad (13)$$

When the surface tension can be neglected:

$$\tau_r = 3\,\tau'_g \frac{1 + y}{\eta' - y}. \quad (14)$$

The basic equation (4) can be rewritten in two different ways, useful for future discussions:

$$-\text{As } P_b = X_b \left(P_0 - \rho g z + \frac{2\sigma}{r}\right),$$

$$\frac{dn}{dt} = sP_0 k r^2 (X_w - X_b (1 + y)). \quad (15)$$

Moreover, $P_b = nRT/V$. Thus,

$$\frac{dn}{dt} + \frac{n}{\tau_g} = sP_0 X_a k r^2 (1 + x). \quad (16)$$

According to the first assumption, at the begin-

ning of its life, the bubble is found at its initial depth in the same composition as the atmosphere from which it is formed. Consequently, when $t = 0$, $X_b = X_a$ and

$$n\,(t=0) = n_0 = \frac{4\pi}{3RT} X_a r_0^3 \left(P_0 - \rho g z_0 + \frac{2\sigma}{r_0}\right). \quad (17)$$

$q\,(t) = n_0 - n\,(t)$ is the amount of gas transferred by a bubble at time t; q is positive when the exchange takes place from the bubble to the water.

2.2. Variation with time in bubble radius and its implications for gas transfer

In this section, we shall describe the mechanisms governing the evolution in the radius during the lifetime of a bubble and question their relative importance.

The variation in the radius during the life of a bubble is controlled by the competition between the tendency towards an increase due to the bubble ascent (τ_p) and the tendency towards a decrease due to air exchange (τ'_g). Fig. 3 shows the relationship between the time constants τ'_g and τ_p, and the radius.

For small radii, $\tau'_g \sim r/k' \to 0$ and $\tau_p \sim 1/w(r) \to \infty$: the variations in the bubble radius are ruled by the gas exchanges and the bubbles tend to dissolve. From eq. (12), as $\eta' \to 0$, $dr/dt < 0$.

In contrast, for large bubbles, because of the predominant influence of the hydrostatic pressure, the bubbles grow:

$$\tau'_g \to \infty \quad \text{and} \quad \tau_p \sim \frac{1}{w(r \to \infty)} = \text{cte}.$$

In this case, it is found that $dt/r \simeq -\frac{1}{3} dP/P$ which is equivalent to $PV = nRT = \text{cte}$.

Fig. 4 shows the depth z_d for which the instantaneous variation in the radius is equal to zero: $dr/dt = 0$.

Using eq. (12),

$$y_d \simeq -\frac{\rho g z_d}{P_o} = \eta'. \quad (18)$$

If the initial depth of a bubble is small enough and $y(t = 0) = y_0$ satisfies $y_0 < \eta'$, during the bubble lifetime, the radius tends to increase. These bubbles are represented by the points under the curves of Fig. 4. In contrast, the points above the curves define the domaine of large depths where bubbles tend to dissolve. As already seen in Fig. 3, the rôle played by hydrostatic pressure compared to the one played by air exchange, increases with the radius. Consequently, larger depths are needed to dissolve large bubbles. Moreover, as dirty bubbles exchange air less efficiently than clean bubbles, their dissolution is more difficult and z_d becomes larger.

Finally, to discover whether the variations in the radius are significant, $|\tau_r|$ must be compared to τ_1. This comparison is shown in Fig. 5. The following

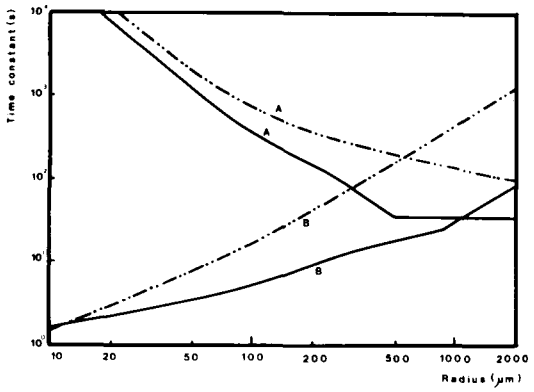

Fig. 3. Variation with the radius r in the time constants τ_p (A) and τ'_g (B). ——: clean bubble; —··—: dirty bubble.

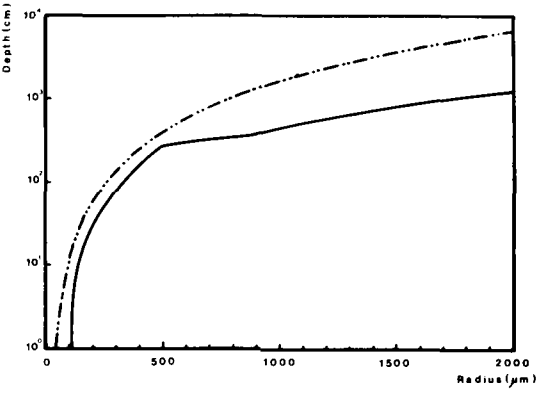

Fig. 4. Variation with the radius r in the depth z_d for which $dr/dt = 0$. ——: clean bubble; —··—: dirty bubble.

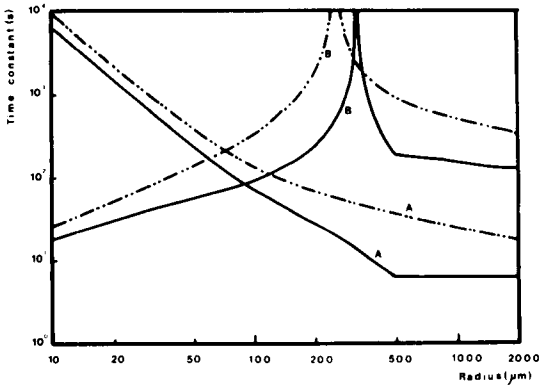

Fig. 5. Variation with the radius r in the time constants τ_1 (A) and $|\tau_r|$ (B). On the left part of the curves B, τ_r is negative: the air transfer term is prevalent and the bubble tends to dissolve. In contrast, on the right part, τ_r is positive: the influence of the decrease in the hydrostatic pressure becomes dominant. The dotted lines represent the cut-off radii r_c: for smaller radii, $\tau_r < 0$ and $|\tau_r| < \tau_1$ i.e. the bubble dissolution is faster than its ascent. Thus the bubble entirely dissolves before reaching the surface.

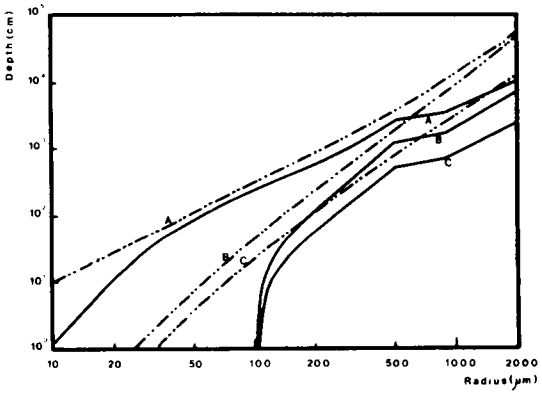

Fig. 6. Variation with the radius r in the limit depths z_c (A) and z_d (B) defined in the text. ——: clean bubble; —·—: dirty bubble.

points can be made:

— for large radii,

$$\tau_r \simeq 3\,\frac{1+y}{y}\,\tau_1 = 3\,\tau_p\,(1+y) > 3\,\tau_p.$$

Thus, assuming $y < 1$ (that is to say $|z_0| < 10$ m), the relative increase of the large radii due to the hydrostatic pressure is always lower than 15%.

— There is a cut off radius r_c for which $\tau_r \simeq -\tau_1$. Bubbles with a radius smaller than r_c entirely dissolve before reaching the surface.

Using eqs. (10) and (14), we can define a depth z_c ($y_c = -\rho g z_c / P_0$) associated with the radius r_c:

$$y_c^2 - 4\,y_c\,\eta' - 3\,\eta' = 0. \tag{19}$$

If the surface tension is taken into account,

$$y_c^2 + y_c(-4\,\eta' + y_\sigma) - \eta'(3 + 2y_\sigma) = 0 \tag{20}$$

with $y_\sigma = 2\sigma / P_0 r_c$.

Fig 6 summarizes the general evolution of bubbles: for a given radius r:

— If the initial depth z_0 is large, that is to say $y_0 = -\rho g z_0 / P_0$ satisfies $y_0 > y_c$, the bubble tends to dissolve: $\tau_r < 0$. Moreover, as $|\tau_r| < \tau_1$, the bubble entirely dissolves before reaching the surface.

— For middle-range initial depths, i.e., $y_c < y_0 < y_d$, the bubble radius decreases between y_0 and y_d, then increases for smaller depth. The bubbles reach the surface: $|\tau_r| > \tau_1$.

— For small depths, when $y_0 < y_d$, the bubbles grow during their whole lifetime.

As a first approximation, we shall use the simplified assumptions: when $|z| > |z_c|$, the bubbles dissolve.

All the gas which was in the bubble is exchanged and:

$$Q = n_0 = N_0\,(1 + y_0),$$

where

$$N_0 = \frac{4\pi r_0^3 P_0 X_a}{3RT}: \tag{21}$$

— when $|z| < |z_c|$, the bubble radius is constant. The integration of eq. (16) gives:

$$Q = N_0\,(y_0 - x)\,(1 - e^{-\tau_1/\tau_g}) \tag{22}$$

2.3. Total amount of gas transferred during the lifetime of a bubble

In this section, we shall first show the general assumptions which can be drawn from approximations 21 and 22, then we shall present the numerical results of the exact integration of eqs. (4) and (9).

2.3.1. Generalities. Eqs. (2) and (22) are the results of approximations: they make possible the presentation of the main points on the variations in the total amount of gas transferred with the principal parameters. The two important terms involved in this study are the ratio τ_1/τ_g, which defines the distance with regard to equilibrium of a bubble

reaching the surface and y_0, which represents the overpressure prevailing in a bubble at the beginning of its life.

By definition,

$$\tau_1/\tau_g = -\frac{3\alpha k z_0}{4\pi r w} = \alpha R_\tau. \quad (23)$$

The higher this ratio is, the closer to equilibrium the bubble is at the end of its life. R_τ increases when the radius decreases. Consequently, medium size bubbles which do not dissolve are in equilibrium when they reach the surface. As R_τ is large.

$$1 - e^{-\alpha R_\tau} \sim 1 \quad \text{and} \quad Q \simeq N_0 (y_0 - x). \quad (24)$$

For large bubbles, R_τ decreases and

$$Q \simeq \alpha N_0 (y_0 - x) R_\tau. \quad (25)$$

Thus, when r_0 becomes large, $Q \sim r_0^{5/2}$. The total amount of gas transferred increases with the initial radius. R_τ is proportional to k/w: this ratio is larger for clean bubbles and they exchange gas more efficiently than dirty bubbles. Finally, as $\tau_1/\tau_g \sim \alpha D^m$ with $m = \frac{1}{2}$ for clean bubbles and $m = \frac{2}{3}$ for dirty bubbles, Q increases with the solubility and with the molecular diffusion coefficient.

The total dissolution of small bubbles (eq. (21)) and the existence of the term y_0 in eq. (22), show that gas invasion into water is favoured compared to gas evasion. When there is equilibrium in solubility (defined by $X_w = X_s$ or $x = 0$), there is no gas transfer across a flat interface. On the contrary, because of the overpressure, equilibrium in solubility implies a positive gas flux from the bubble to the water. Moreover, even with a supersaturated water for which $0 < x < y_0$, there is gas invasion into the water. When bubbles are considered, there is no symmetry between evasion and invasion.

2.3.2. Numerical results. Fig. 7 and 8 show the relationship between the total amount of gas transferred and the initial radius, for clean and dirty bubbles. The gas considered is defined by its molecular diffusion coefficient D, its solubility s and $X_a = X_w = 10^{-5}$.

The general ideas presented in the previous paragraph by means of simplified assumptions are verified. However, for large solubilities, when $\alpha = sRT \geqslant 0.1$, the total amount of gas transferred is not systematically increasing with α or D and even dirty bubbles can exchange more trace gas than clean bubbles.

This phenomenon can be better understood with the help of Fig. 9. When the solubility is large, the sign of the gas flux can change during the bubble ascent. This effect cannot be explained assuming the radius to be constant. In this case, the integration of eq. (16) shows that the sign of dn/dt is given by the sign of $(x - y_0)$. This means that the sign of the gas flux is determined by the initial conditions. At the beginning of its life, if the overpressure y_0 is more important than the saturation indicator x, the bubble will always lose gas. As a matter of fact, when the gas is very

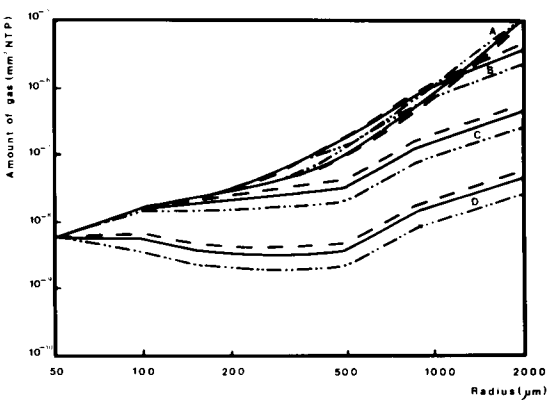

Fig. 7. Relationship between the amount of gas transferred during the lifetime of a bubble Q and the bubble radius r. Clean bubble, $X_a = X_w = 10^{-5}$, $z_0 = -100$ cm. A: $\alpha = 1$; B: $\alpha = 0.1$; C: $\alpha = 0.01$; D: $\alpha = 0.001$. $\alpha = sRT$ where s is the gas solubility. —·—·—: $D = 10^{-5}$; ——: $D = 3 \times 10^{-5}$; – – –: $D = 5 \times 10^{-5}$. D (cm$^2 \cdot$ s^{-1}) is the gas molecular diffusion coefficient.

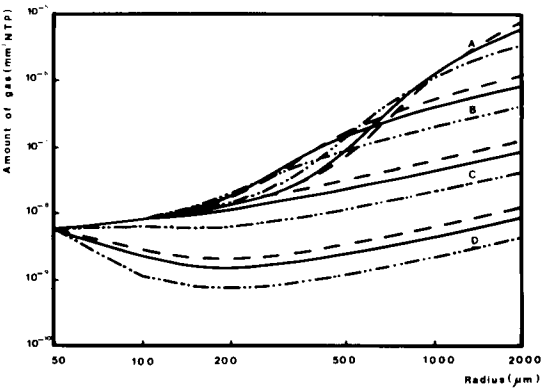

Fig. 8. Same as on Fig. 7 for dirty bubble.

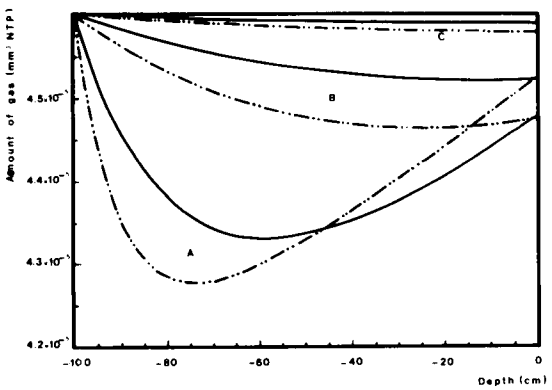

Fig. 9. Variation with depth of the amount of trace gas contained in the bubble during the bubble life. Clean bubble, $X_a = X_w = 10^{-5}$, $r_0 = 1000\ \mu m$, $z_0 = -100$ cm. A: $\alpha = 1$; B: $\alpha = 0.1$; C: $\alpha = 0.01$; $\alpha = sRT$ where s is the gas solubility. ——: $D = 10^{-5}$; — · · —: $D = 5 \times 10^{-5}$; D ($cm^2 \cdot s^{-1}$) is the molecular diffusion coefficient.

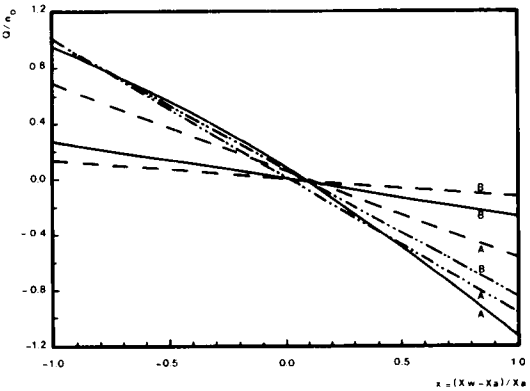

Fig. 10. Variation with the water saturation indicator x in the amount of gas transferred during the lifetime of the bubble, weighted by the initial amount of gas contained in the bubble n_0. Clean bubble, $z_0 = -100$ cm. A: $r_0 = 200\ \mu m$; B: $r_0 = 500\ \mu m$. ——: O_2; — · · —: CO_2; – – –: He.

soluble, the phenomena are more intricate. In the examples shown in Fig. 9, as $x = 0$, the bubble starts its ascent losing gas. If the value of α is high, it tends very rapidly to reach the equilibrium for the trace gas considered; the gas exchange constant time τ_g is very small. Then it continues its ascent to the surface. Because of the resulting decrease in the overpressure y, it becomes relatively too poor with respect to this trace gas. Consequently, during the second part of its life, the bubble absorbs this gas.

Eq. (22) suggests that the relationship between the total amount of gas transferred and the difference $c - sP_a$ ($= sP_o X_a x$) where c is the gas concentration in water and P_a the gas partial pressure in the atmosphere (and *not in the bubble*) is linear. Fig. 10 confirms this idea, at least for trace gases (He and CO_2). The behaviour of a bubble is directly linked to the transfer of the air gases O_2 and N_2. Because of the relatively large amounts of these gases, small variations in their concentrations in water can have significant impacts on the evolution of the bubble radius. Gases in small quantity do not exercise a large influence on the radius variations. Consequently, in the case of trace gases, as r, and thus τ_g and k, does not depend on x, eq. (16) shows that n and thus Q, is a linear function of x, even if the radius is not assumed to be constant.

2.3.3. Conclusion. Before taking up the gas transfer by a bubble population, we would like to summarize and point out some general rules governing the gas exchange through a single bubble.

— As a first approximation, when a bubble does not dissolve entirely, its radius can be assumed to be constant during its lifetime.

— Generally the total amount of gas transferred increases with the initial radius, the molecular diffusion coefficient and the solubility.

— For gases with low solubility, clean bubbles transfer much more gas than dirty bubbles. However, there is no large difference between the gas exchanged by clean and dirty bubbles when solubilities are high.

— The relationship between the total amount of gas transferred Q and the difference of gas concentrations, $c - sP_a$ between the water and the surface is linear.

3. Theory of gas transfer for a bubble distribution

3.1. General equations

In the following, all the parameters concerning the bubble distributions are horizontally averaged: z is the only spatial parameter. Moreover a steady state regime is assumed: the bubble source does not change with time.

3.1.1. Definitions. A bubble distribution is known in terms of bubble radius and depth. The instan-

taneous gas flux through a bubble also depends on the partial pressures of the gases considered in the bubble (see eq. (4)).

Once the different gas concentrations in water and in air are known, a bubble is entirely described by its initial radius r_0, its initial depth z_0 and the time elapsed since it has been created t. Let us consider the function $\Phi(r_0, z_0, t)$ defined such that $\Phi(r_0, z_0, t)\mathrm{d}r_0\mathrm{d}z_0\mathrm{d}t$ represents the number of bubbles in the volume element $\mathrm{d}^3v = \mathrm{d}r_0\,\mathrm{d}z_0\,\mathrm{d}t$ about (r_0, z_0, t). If $\mathrm{d}n/\mathrm{d}t\,(r_0, z_0, t)$ is the instantaneous flux through the bubble. (r_0, z_0, t), the total flux is then defined by:

$$F_B = \int\int\int \Phi(r_0, z_0, t)\,\frac{\mathrm{d}n}{\mathrm{d}t}\,(r_0, z_0, t)\,\mathrm{d}r_0\mathrm{d}z_0\mathrm{d}t. \qquad (26)$$

Because of the steady state regime, Φ is also the number of bubbles created about (r_0, z_0) during $\mathrm{d}t$, i.e., $\Phi(r_0, z_0, t) = S\,(r_0, z_0)$, where S is the bubble source distribution, independent of time. After integrating eq. (26) with time, it follows that:

$$F_B = \int\int S\,(r_0, z_0)\,Q\,(r_0, z_0)\,\mathrm{d}r_0\,\mathrm{d}z_0. \qquad (27)$$

3.1.2. Bubble transport equation. Garrettson (1973) has set up the equations coupling source and distribution through bubble dynamics. Assuming a steady state regime,

$$w\frac{\partial\psi}{\partial z} + \gamma\frac{\partial\psi}{\partial r} + A_r\,\psi = S, \qquad (28)$$

where $\psi\,(r, z)$ is the bubble distribution and

$$\gamma = \frac{\mathrm{d}r}{\mathrm{d}t}, \qquad A_r = \frac{\partial\gamma}{\partial r}.$$

γ is given by eq. (9) and makes eq. (28) hardly usable. The previous study on the variation in radius during the lifetime of a bubble introduced a cut-off radius: the radius of larger bubbles can be assumed to be constant. In order to simplify eq. (28) and to be able to use it, the terms taking into account the variation in the radius will be neglected.

Eqs. (9) and (28) can give some information on the consequences of this simplification. For large bubbles, the dominance of the hydrostatic pressure term over the air exchange term implies an increase in the radius. Consequently, for a given bubble distribution ψ, the bubble source is slightly overestimated. In contrast, in the range of small bubbles, the decrease in the radius due to the air transfer can become important: in this case, S_0 is underestimated. This effect is weighted by the fact that $Q\,(r_o, z_0)$ decreases quickly with r_0 ($Q \sim r_0^3$ for dissolving bubbles): the importance of small bubbles in the flux defined by eq. (27) is not great.

With these assumptions, eq. (28) turns out to be equivalent to :

$$S = w\frac{\partial\psi}{\partial r}. \qquad (29)$$

In situ measurements of bubble populations are not so numerous. Data reviewed by Wu (1981) show that the general shape of a bubble distribution can be roughly represented by:

$$\psi = \psi_0 f(u)\,\mathrm{e}^{z/L}\,r^{-a},$$

with $3 < a < 5$ and $L \sim 1$ m. This relationship is valid for radii larger than $60 - 80\,\mu$m: indeed, the measurements show a rapid drop off toward small sizes.

The relationship between ψ and the wind velocity obtained by Wu with different data satisfies $f(u) \simeq u^{4.5}$. Using a linear function between the wind stress coefficient $C_D = (u_*/u)^2$ (where u_* is the friction velocity) and the wind velocity (Wu, 1982), it is found that $\psi \sim u_*^3$.

3.1.3. Global gas flux and transfer velocity. Using eqs. (27) and (29), the total gas flux for a bubble distribution is given by:

$$F_B = \int\int w(r)\,\frac{\partial\psi(r, z)}{\partial z}\,Q\,(r, z)\,\mathrm{d}r\,\mathrm{d}z. \qquad (30)$$

From the definition of transfer velocity, the gas flux F_T per surface unit is equal to the product of the transfer velocity k_L and the difference of concentrations between the interface, c_e ($=sP_a$: Henry's law) and the bulk water, c.

When there are no bubbles, $F_T = F_S = -k_S\,(c - sP_a)$. Using the parameters presented earlier,

$$F_S = -k_S sP_0X_a x = -k_S P_0 X_a \alpha x/RT = -F_A\,\alpha x. \qquad (31)$$

It is important to remember that the transfer velocity k_S is a parameter depending only on the Schmidt number $\mathrm{Sc} = \nu/D$ of the gas considered and on the hydrodynamic conditions of the air-water interface.

At high wind speeds, when the breaking waves create bubbles, the total flux is the sum of the flux through the bubbles F_B and of the flux across the

sea surface F_S: $F_T = F_S + F_B$. Thus,

$$k_L = -\frac{F_s}{(c - sP_a)} - \frac{F_B}{(c - sP_a)} = k_S + k_B.$$

Consequently, the transfer velocity of the bubbles is defined by:

$$k_B = -\frac{\int\int w\,(\partial\psi/\partial z)\,Q\,dr\,dz}{(c - sP_a)} \qquad (32)$$

This is exactly the term measured in situ and during wind tunnel experiments (Siems, 1980; Merlivat and Memery, 1983). We can remark that k_B is not the mean of the transfer velocities of the bubbles weighted by their surfaces.

3.2. *Gas flux at the air-water interface*

In the following, the bubble distribution is given by:

$-\psi \sim \exp(+z/L)$ $\quad z < 0$ (in meters) and $L = 1$ m;

$-\psi \sim r^{-4}$ $\quad$ when $r > 75\ \mu$m;

$\psi = \text{cte}$ $\quad$ when $r < 75\ \mu$m.

The number of bubbles is equal to 10^4 bubbles/l at $z = 0$ m.

According to Wu's data, this distribution represents some sample distribution with a mean value of a. The fact of choosing ψ to be constant in terms of the radius for small bubbles takes into account the rapid drop off towards small sizes. The relationship between the bubble population and the radius is not very critical for small radii, according to the convergence of the integral (30): as bubbles dissolve entirely, $w(r)\,Q(r,z) \sim r^5$. Another choice for the bubble distribution has no consequence for the discussion and in the general ideas presented below, only the numerical results should be changed.

3.2.1. General shape of the function F_B (x); Role of the solubility. Fig. 11 shows the relationship between the gas flux through bubbles F_B and the ratio $x = (X_w - X_a)/X_a$ for different gases.

In Subsect. 2.3.2., it has been seen that the total amount of trace gas transferred by a single bubble varies linearly with x. Consequently, the integration of these quantities with the bubble source satisfies the same relationship. Of course, this is not the case for the main air gases, like O_2.

In spite of the limitation of eq. (22) studied

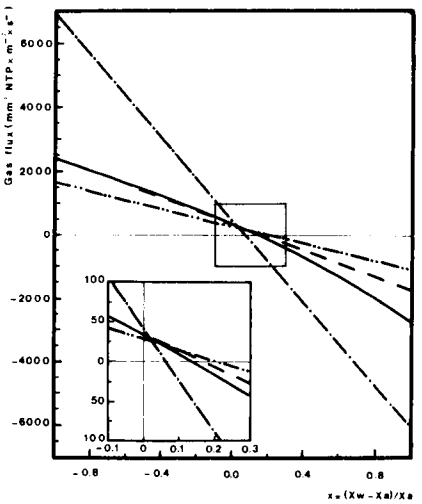

Fig. 11. Variation in the total gas flux through bubbles F_B with the water saturation indicator x. Bubble distribution presented in the text. —·—·—: He; – – –: Ar; —·—·—: CO_2; ——: O_2. The intersection of the curves with the x-axis gives the x value, x_0 of the water saturation for which $F_B = 0$: the flux water → large bubbles is counterbalanced by the flux small bubbles → water.

previously (in Subsect. 2.3.2.), this equation, when combined with eq. (21), gives a good idea of the variations in the total gas flux F_B. In order to simplify this, bubbles which do not dissolve can be separated into two groups, already presented by eq. (24) (medium sized bubbles) and (25) (large bubbles):

$$F_B = \int\int_{\Delta_1} N_0(1 + y_0)\,dr\,dz + \int\int_{\Delta_2} N_0(y_0 - x)\,dr\,dz + \alpha \int\int_{\Delta_3} N_0\,(y_0 - x)\,R_\tau\,dr\,dz, \qquad (33)$$

$\Delta_1 = \{\text{entirely dissolving bubbles}\}$

$\Delta_2 U \Delta_3 = \{\text{bubbles arriving to the surface}\}$ with

$\Delta_2 = \{\text{bubbles reaching the equilibrium}\}$

$\Delta_3 = \{\text{bubbles not reaching the equilibrium}\}$;

$$F_B = \int\int_{\Delta_1} N_0\,(1 + y_0)\,dr\,dz + \int\int_{\Delta_2} N_0 y_0\,dr\,dz + \alpha \int\int_{\Delta_3} N_0 y_0 R_\tau\,dr\,dz$$

$$- x\left(\int\int_{\Delta_2} N_0\,dr\,dz + \alpha \int\int_{\Delta_3} N_0 R_\tau\,dr\,dz\right) = F_p - xF_x. \qquad (34)$$

Approximation (34) agrees with the linear relationship between F_B and x of Fig. 10. Moreover, eq. (34) shows that the slope of the line F_B (x), and

thus the flux itself, increases with the solubility. We can remark that the dependency between F_B and α is only due to the influence of the large bubbles. For smaller bubbles, the transfer kinetics are fast enough to not influence the gas flux; thus the limit conditions (total dissolution or equilibrium) are reached.

3.2.2. Supersaturation of the water. One of the main differences between a bubble population approach and an air-water interface approach is clearly perceptible when eqs. (31) and (34) are compared. The flux across a flat air-water interface F_S is proportional to x, i.e., to $X_w - X_a$ or $c - sP_a$, which is not the case for the flux through bubbles F_B. In eq. (34), F_p represents the rôle played by the hydrostatic pressure and by the surface tension which tends to dissolve the bubbles and to favour the gas invasion into the water: a gas in equilibrium in solubility ($x = 0$ or $c = sP_a$) is not exchanged across the flat air-water interface but is nevertheless transferred from the atmosphere into the water by means of bubbles, F_B is equal to 0 for a supersaturation of the gas in the water:

$$x_0 = \frac{F_p}{F_x} > 0.$$

Table 2 presents some x_0 values for different gases and for the bubble distribution used: x_0 increases when the solubility decreases or when the bubbles are dirty.

The actual equilibrium is obtained when the total flux $F_T = F_S + F_B$ becomes equal to zero. The associated value x_{eq} is given by:

$$x_{eq} = \frac{F_p}{F_x + \alpha F_A}; \qquad (35)$$

$$0 < x_{eq} < x_0.$$

When $x = x_{eq}$, a steady state is obtained: the gas flux from the bubbles to the water ($x_{eq} < x_0 \Rightarrow F_B > 0$) is balanced by an opposite flux across the air water interface ($x_{eq} > 0 \Rightarrow F_S < 0$). The less soluble the gas is, the more supersaturated the water is. Some examples with different trace gases are shown in Fig. 12. Dirty bubbles are less efficient than clean bubbles. Consequently their contribution in the total gas exchange is less significant and the supersaturation at equilibrium is lower.

3.2.3. Transfer velocity. During gas transfer experiments in wind-wave facilities or during in situ measurements, the parameter obtained is the

Table 2. *Fluxes and transfer velocities computed for different gases with the bubble distribution defined in the text*

	Clean bubble				Dirty bubble			
	CO_2	Rn	Ar	He	CO_2	Rn	Ar	He
$\frac{F_p}{X_a}$*	414	464	353	279	101	95	75	66
$\frac{F_x}{X_a}$*	6,466	4,776	2.068	1,228	1,338	850	409	295
x_0 ($\times 100$)	6.4	9.7	17.1	22.7	7.6	11.2	18.4	22.5
k_B ($x = -1$)†	2.8	7.8	24	63	0.59	1.4	4.7	15
k_B ($x = 1$)†	2.5	6.4	17	39	0.51	1.1	3.3	9.5
k_B (He)/k_B‡	22.5	8.1	2.6	—	25.4	10.7	3.2	—
$\frac{k_B \text{ (clean)}}{k_B \text{ (dirty)}}$‡	4.7	4.6	5.1	4.2	—	—	—	—

The bubble flux F_B is equal to $F_p - xF_x$ with $x = (X_w - X_a)/X_a$, x_0 is defined by $F_B(x_0) = 0$. The transfer velocity k_B is given by $k_B = -F_B/sP_0X_a x$. x_0 and the differences between k_B ($x = -1$) and k_B ($x = 1$) show the influence of the overpressure prevailing in the bubbles, k_B (He)/k_B the influence of the physico-chemical properties (above all the solubility) of the gas and k_B (clean)/k_B (dirty), the influence of the surfactants.

* In mm^3 NTP $\cdot m^{-2} \cdot s^{-1}$.

† In $cm \cdot h^{-1}$.

‡ Ratios computed for $x = -1$.

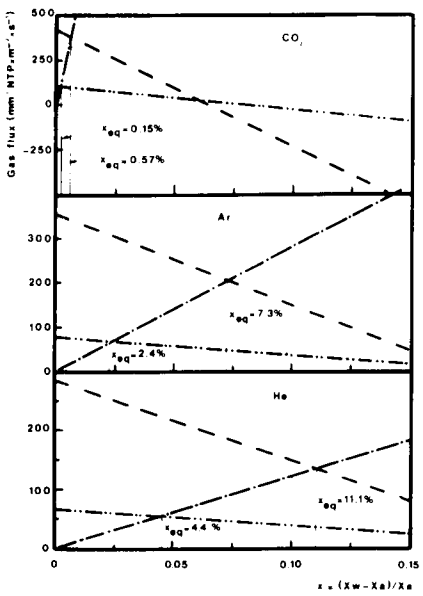

Fig. 12. Variation in different gas fluxes with the water saturation indicator x. —·—: $-F_S$ is given by eq. (33) and is computed using $k_S = 50$ cm h^{-1} for CO_2 and assuming that $k_S \sim S_c^{-1/2}$ in the calculations for Ar and He. ---: F_B for clean bubbles; —··—: F_B for dirty bubbles. F_B is computed with the bubble distribution of the text. The intersection of F_B and $-F_S$ gives the x value, x_{eq} for which $F_B + F_S = 0$, i.e., for which there is equilibrium: the gas flux from the bubbles to the water counterbalances the evasion across the air-water interface.

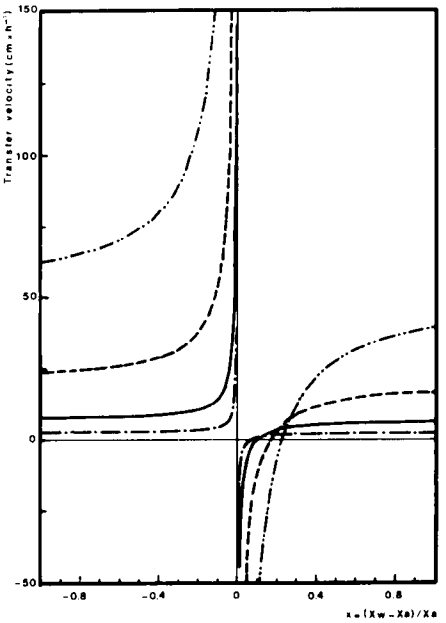

Fig. 13. Variation in the transfer velocity through bubbles k_B with the water saturation indicator x. —·—: CO_2; ——: Rn; - - - -: Ar; —··—: He.

transfer velocity k_L, the sum of k_S and k_B. The main conclusions proceed directly from the eq. (32). Fig. 13 represents the variation in k_B in terms of x for different gases.

Using the approximation (34):

$$k_B = -\frac{k_p}{x} + k_x, \tag{36}$$

with

$$k_p = +\frac{F_p}{sP_0X_a}, \qquad k_x = \frac{F_x}{sP_0X_a}.$$

The general shape of the curves of Fig. 12 can be explained by eq. (36):

— there is a singularity when $x = 0$;

— when $0 < x < x_0$, the transfer velocity is negative: the gas flux F_B and the difference of concentrations $c - sP_a$ have same signs;

— far from equilibration, k_B becomes x-independent:

$$k_B \xrightarrow[x \to \infty]{} k_x.$$

Using eq. (34), k_x can be written: $k_x = a + b/s$. The transfer velocity increases when the solubility decreases;

— the difference between evasion and invasion is clearly shown by the following limit conditions:

$$k_B\,(x \to \infty) = k_x,$$
$$k_B\,(x \to -1) = k_x + k_p.$$

In the same way as k_x, k_p increases when s decreases: the non-symmetry between evasion and invasion is all the more important as the solubility is low.

3.2.4. Conclusion. This study has shown the difference in nature and behaviour between the gas flux across an air-water interface F_S and the flux through a bubble population F_B. By definition, F_S is directly proportional to the solubility and to the difference of concentration $c - sP_a$ (i.e., to the saturation indicator $x = (X_w - X_a)/X_a$). In the contrast, while F_B varies linearly with these two parameters, it is not proportional to solubility

because the transfer kinetics through small and medium size bubbles are very fast and the exchange is entirely developed up to dissolution or equilibrium. It is not proportional to the saturation indicator because of the overpressure prevailing in the bubbles which favours invasion; thus, the actual equilibrium is obtained for a supersaturation of the water in gas, which is all the more significant when the solubility is low.

The consequences for the transfer velocity k_B are very important: on the one hand, the solubility is a physico-chemical parameter which, as the Schmidt number, must be taken into account in the k_B definition; on the other hand, the behaviour of k_B makes it hardly usable, above all near the equilibrium in solubility. In nature, radon is always found in evasion conditions and $x \to \infty$: it is thus possible to use the notion of transfer velocity, even when there are bubbles. In contrast, for CO_2, x varies between -0.1 and $+0.1$ (Takahashi and Azevedo, 1982). Therefore, the use of a Schmidt number dependency alone to compute the CO_2 exchange with the help of radon measurements is questionable. Not only is the solubility an important parameter, but the CO_2 concentration in water must also be taken into account.

4. General conclusions and prospects

This study has presented the general equations governing gas flux through bubbles and has allowed us to gain some insight in the understanding of the mechanisms involved. Nevertheless, several points remain unsolved by the development presented here.

The dependency between transfer velocity k_L and wind velocity u is of particular importance. Wu's data indicate that the bubble contribution, and thus the gas flux, increases with u and satisfies the relationship: $\psi \sim u^{4.5}$ ($\sim u_*^3$). Until now, the only studies which allow a correlation between k_L and u when there are breaking waves are the Siems experiments. At this time, they seem to show a linear relationship between transfer rate and wind velocity. It is obvious that more measurements are needed.

Mainly two parts of the model can be improved: the description of water dynamics and the resolution of the bubble transport equation.

The flow under a breaking wave is not very well-known. Thorton (1979) has shown that the average velocity intensity in the surf zone is 85% wave induced. Using photographic techniques to follow bubble trajectories, Toba et al. (1975) and Koga (1982) have visualized the convection accompanying breaking waves. At the lee face of the wave crest, the surface water converges and air bubbles are entrained by a downward flow. They rise up to the surface at the rear side of the wave. This general pattern is roughly taken into account by Thorpe (1982) in his model of gas transfer by bubbles. Orbital motions of Stockes are introduced in the computations run by Merlivat and Memery (1983). Comparisons with the revised model presented here show that the increase in gas exchange consequent upon the change in bubble dynamics due to orbital motions is about 15%, which is not significant with regard to the influence of surfactants. As a first approximation, downward convection, turbulence created by breaking waves and orbital motions imply first of all an increase in the bubble lifetime. Table 3 gives some results on the influence of this increase of bubble lifetime, which is assumed to be the same for every bubble. Bubbles dissolving entirely or reaching equilibrium (eq. (33)) are not affected. Consequently the CO_2 transfer which is fast for any bubble does not depend significantly on the hypotheses determining the bubble lifetime. This is not the case for He or Ar: their solubilities being low, most of the bubbles arriving at the surface are far from equilibrium and

Table 3. *Influence of an increase Δt in the bubble lifetime on gas transfer*

		CO_2	Rn	Ar	He
$\Delta t = 0$	$k_b\,(x = 1)$*	2.8	7.8	23.4	60.4
	$k_b\,(x = -1)$*	2.2	5.9	16.9	42.6
$\Delta t = 1$ s	$\Delta\,(x = 1)$†	2.5	9.6	13.5	13.8
	$\Delta\,(x = -1)$†	2.8	10.9	15.3	15.9
$\Delta t = 5$ s	$\Delta\,(x = 1)$†	4.3	26.4	57.0	59.0
	$\Delta\,(x = -1)$†	4.9	29.8	64.7	67.6

Δt is the same one for every bubble. The amounts of gas transferred are computed using the approximations 21 and 22. Case of clean bubbles.

* In $cm \cdot h^{-1}$.

† Δ is the relative change (%) in k_b for a given Δt with respect to k_b obtained for $\Delta t = 0$.

x is the saturation indicator defined by $x = (X_w - X_a)/X_a$ where X_w and X_a are the gas mole fraction in the water and in the air, respectively.

the bubble lifetime value plays a major rôle (eq. (25)).

When the variation in bubble radius with time is taken into account, the transport equation (eq. (28)) is hardly usable without drastic simplifications (which are not necessarily more justified than neglecting the terms concerning the variation in bubble radius). Moreover eq. (27), directly coupling flux through bubbles and bubble source distribution, shows that the use of the bubble transport equation is avoidable if the source distribution is known. Finally, rather than a universal bubble distribution, it is surely safer to imagine a universal bubble source spectrum defined by parameters describing the hydrodynamical conditions at the air-water interface. Based on dimensional analysis and on the hypothesis of mass continuity (the mass of air bubbles produced per unit area per time at any radial scale is independant of radius), Kerman (1982) has proposed a first approach to this problem. The relationship obtained which defines the bubble source is given by $S \sim u_*^2 r^{-3}$. Using eq. (29), which gives the relationship between bubble source and bubble distribution through bubble dynamics, this result is in good agreement with the data on bubble distributions presented by Wu. Nevertheless, the model is only valid in the range of large radii where the rôle of the hydrostatic pressure is predominant in the variation in bubble radius: it does not consider the air transfer and the dissolution of small bubbles. Another problem exists. We already know that $Q \sim r^{5/2}$ for large bubbles, which implies that using Kerman's relationships $QS \sim r^{-1/2}$ which does not converge when the radius increases: the gas flux through bubbles should be infinite! Other theoretical developments on this matter are necessary and will be very useful for a complete parameterization of the gas transfer across the atmosphere-ocean interface. The source distribution must be quantified with the help of general synoptic data of the ocean surface obtained from satelite measurements.

5. Acknowledgments

The authors are particularly indebted to Dr. B. R. Kerman for valuable discussion and helpful criticisms. They thank J. White for useful comments on the paper.

REFERENCES

Batchelor, G. K. 1967. *An introduction to fluid dynamics*. Cambridge University Press, 615 pp.

Broecker, W. S. and Peng, T. H. 1974. Gas exchange rates between air and sea. *Tellus 26*, 21–35.

Deacon, E. L. 1977. Gas transfer to and across an air-water interface. *Tellus 29*, 363–374.

Garrettson, G. A. 1973. Bubble transport theory with application to the upper ocean. *J. Fluid. Mech. 59*, 187–206.

Hasse, L. and Liss, P. S. 1980. Gas exchange across the air-water interface. *Tellus 32*, 470–481.

Jahne, B., Huber, W., Dutzi, A., Wais, T. and Ilmberger, J. 1984. Wind-wave-tunnel experiment on the Schmidt number and wave field dependence of air-water gas exchange. In *Gas transfer at water surfaces* (eds. Brutsaert and Jirka). Dordrecht: D. Reidel Publishing Company, 303–310.

Kerman, B. R. 1982. Distribution of bubbles near the ocean surface, Report AQRB-82-008-L, Boundary Layer Research Division, Downsview, Ontario, Canada.

Kerman, B. R. 1984. A model of interfacial gas transfer for a well roughened sea. *J. Geophys. Res. 89*, D 1, 1439–1446.

Koga, M. 1982. Bubble entrainment in breaking wind waves. *Tellus 34*, 481–489.

Levich, V. G. 1962. *Physicochemical Hydrodynamics*. Prentice Hall, Englewood-Cliffs, N.J., 700 pp.

Merlivat, L. and Memery, L. 1983. Gas exchange across an air-water interface: experimental results and modeling of bubble contribution to transfer. *J. Geophys. Res. 88*, C1, 707–724.

Takahashi, T. and Azevedo, A. E. G. 1982. The oceans as a CO_2 reservoir. In *Interpretation of climate and photochemical models, Ozone and temperature*. Am. Inst. Phys., N.Y., 83–109.

Thornton, E. B. 1979. Energetics of breaking waves within the surf zone. *J. Geophys. Res. 84*, C8, 4931–4938.

Thorpe, S. A. 1982. On the clouds of bubbles formed by breaking wind-waves in deep water, and their role in air-sea gas transfer. *Phil. Trans. R. Soc. London. 304*, 155–210.

Toba, Y., Tokuda, M., Okuda, K. and Kawai, S. 1975. Forced convection accompanying wind waves. *J. Oceanogr. Soc. Ja. 31*, 192–198.

Wu, J. 1981. Bubble populations and spectra in near surface ocean: summary and review of field measurements. *J. Geophys. Res. 86*, C1, 457–463.

Wu, J. 1982. Wind-stress coefficients over sea surface from breeze to hurricane. *J. Geophys. Res. 87*, C12, 9704–9706.

Yaglom, A. M. and Kader, B. A. 1974. Heat and mass transfer between a rough wall and turbulent fluid flow at high Reynolds and Peclet numbers. *J. Fluid Mech. 62*, 601–623.